

# ALS-P: Light Weight Visible Light Positioning via Ambient Light Sensor

Zeyu Wang\*, Zhice Yang<sup>†</sup>, Qianyi Huang\*, Lin Yang<sup>‡</sup>, Qian Zhang\*

\*Computer Science and Engineering, Hong Kong University of Science and Technology, Hong Kong

<sup>†</sup>Shanghai Tech University, P.R. China

<sup>‡</sup>Huawei Noah's Ark Lab, P.R. China

E-mail: zwangas@connect.ust.hk, yangzhc@shanghaitech.edu.cn  
quhuangaa, lyangab@connect.ust.hk, qianzh@cse.ust.hk

**Abstract**—Visible light positioning (VLP) is a promising direction for indoor localization. VLP depends on Visible light communication (VLC) to receive location anchors sent by light bulbs. In order to decode high-frequency VLC signals, today's VLP systems require the receiver to equip either rolling shutter cameras or high-frequency light sensors, which bring considerable overhead or are even unavailable on many mobile devices.

This paper introduces ALS-P, a lightweight VLP approach which only requires the commercially widely available ambient light sensor (ALS). ALS is conventionally not treated as a feasible VLC receiver as its sampling rate is far less than that of VLC signals. Our basic idea is to leverage the property of frequency aliasing. Through dynamically adjusting the sampling rate of the ALS sensor, the down-converted signals can be uniquely distinguished. To realize this idea, we propose novel designs to address challenges which stem from ALS hardware, high-order light aliasing, and environmental interference cancellation. Besides, ALS can also enable a lightweight VLC via changing LED frequencies.

We implement the ALS-P on commercial LED bulbs and the ALS of existing smartphones. The evaluation shows that the ALS-P can enable robust and efficient LED frequency decoding with at least 4LEDs bulbs in practical scenarios. As a result, ALS-P can enable VLC at a data rate of 5bit/s per each LED bulb and achieve a sub-meter level indoor localization accuracy.

## I. INTRODUCTION

In this decade, using ubiquitous lights for data communication is becoming increasingly popular. Visible Light Communication (VLC) typically leverages ceiling LED bulbs serving as transmitters to communicate with smart devices (e.g., smartphones) [1]. One of the most popular applications of VLC is visible light positioning (VLP). VLP uses light bulbs as location anchors, and the localization information is sent from light bulbs through VLC. Then, mobile devices can perform localization if they can decode the location information from the VLC signals of the light bulbs. Since the visible light signal is highly directional, localization through VLP can achieve sub-meter accuracy, which is much better than radio-based methods [2], [3], [4]. As a result, VLP is a promising accurate indoor localization approach in recent literature.

However, today's VLP systems require high-frequency light sensors to decode the high-frequency VLC signal, in which >1000Hz on-off rate is needed to avoid flicking effect. Such light sensors are generally unavailable in current mobile devices. Recent research suggests leveraging the rolling shutter effect of CMOS sensors to capture the high-frequency signals [2]. However, cameras are also not available on many mobile devices like wearables. Further, decoding the rolling shutter effect also brings considerable overheads. Even after the

optimization, the power of the VLC application with a camera is still close to 1Watt [5], which is admittedly not suitable for low power devices.

This paper introduces ALS-P, introduces ALS-P, a lightweight VLP approach. ALS-P utilizes the ambient light sensor (ALS), which is tiny, cheap and widely available. ALS is conventionally not treated as a feasible VLC receiver as its sampling rate is far lower than VLC signals. Our basic idea is to leverage the property of frequency aliasing, i.e., the high-frequency light signal will be aliased to a low frequency when sampled by ALS. By dynamically adjusting the sampling rate of the ALS sensor, the frequency of the high-frequency VLC signals can be uniquely determined by low-frequency samples. On the other hand, to reliably convey location information in the aliased signals, each ALS-P transmitter uses a fixed and unique frequency to represent its location. Then, the VLC receiver can infer its location merely through determining the received frequencies. The location-frequency mapping scheme has another benefit that it is compatible with none-intelligent LED bulbs, which can significantly reduce its deployment cost.

However, challenges emerge when using the ALS as a VLC receiver. The first one stems from the hardware properties of the ALS. Unlike common ADCs, the ALS automatically integrates the sampled light intensity through a specified period. The integration of ALS results in an uneven frequency response to the sampling process, which is quite similar to frequency selective fading in wireless channels. As a result, LED bulbs with specific frequencies have a very low SNR which significantly affects the localization accuracy. Another challenge is the rich interference. Since VLC transmitters are not band-limited, the light signals contain rich harmonics, which can confuse the decoding process. When receiving VLC signals from multiple LED bulbs, this problem becomes very severe. Besides, the fluorescent light which flickers at 50/60 Hz also brings ambiguities in determining the transmitter's frequencies.

To handle those challenges, we propose corresponding designs at both the transmitter and the receiver side. We carefully model and study the integration effect and harmonic interference, according to which we identify a safe zone for the transmitter's frequency selection. To overcome interference from multiple transmitters, we design a novel decoding algorithm in the design of the ALS-P receiver. Based on the observation that the multiple LED bulbs sensed by a receiver must be neighbors, the decoding algorithm will check the relative distance between multiple LEDs when a possible solution is detected. The fluorescent effect is solved based



**Fig. 1: The example of an Ambient Light Sensor**

on the observation that the aliased frequency of it is fixed and the decoding algorithm will also consider the fluorescent light.

We implement the prototype of ALS-P on the ALS of the commercial smartphones, which senses the light signal from commercial intelligent LED bulbs. The localization algorithm of ALS-P is borrowed from existing approaches[3]. Then we evaluate our design based on experiment, and the result shows that (1) ALS-P can decode a frequency higher than 1000Hz with multiple sampling rates up to 100Hz in a variety of environments including different ambient lights and mobility conditions with a low data rate. (2) The transmission range of ALS-P is 4 meters with an SNR higher than 3dB under practical scenarios. (3) The median localization accuracy of the localization prototype is 15cm with 4 LEDs.

The main contributions of ALS-P can be summarized as follows: (1) We observe that ALS can be a VLC receiver to sample high-frequency LED via frequency aliasing effect. The further feasibility study validates our idea. (2) We design ALS-P and propose several schemes for both transmitter and receiver to handle the problem of frequency selection and interference. (3) We implement a prototype of ALS-P and conduct a complete evaluation of it. The experimental results show that ALS-P has a good performance of VLC with various scenarios and interferences and it can achieve a lightweight VLC throughput as 5bit/s per each LED bulb. (4) The localization result shows that ALS-P can enable lightweight indoor localization with sub-meter level accuracy.

## II. OVERVIEW

In this section, we first introduce the working mechanism of ALS and the overhead in the conventional VLC system. We then propose the idea to leverage ALS as the receiver for a lightweight VLC.

### A. Ambient Light Sensor Primer

ALS, as shown in Figure 1, is widely used in mobile devices to provide information about the ambient light level to control the screen brightness automatically.

The sensing part of an ALS is the photo-diode, which converts the intensity of the incidental light into the amplitude of the voltage  $I(t)$ , which is then quantified by the ADC. ALS's output  $A(t)$  is an integration of the intensity values in a period of time of  $T_s$ :

$$A(t) = \int_t^{t+T_s} I(\tau) d\tau, \quad (1)$$

The specific parameter depends on the type of the ALS. Take TMG3992 of AMS AG[6] as example, its minimum integration  $T_s$  is about 2.8ms, and the maximum sampling rate of it is around 100Hz.

A critical feature of ALS is low-power. The total power of ALS is around 1mW at most[6], so many low power devices or applications can continuously obtain data from ALS without worrying about the battery life.

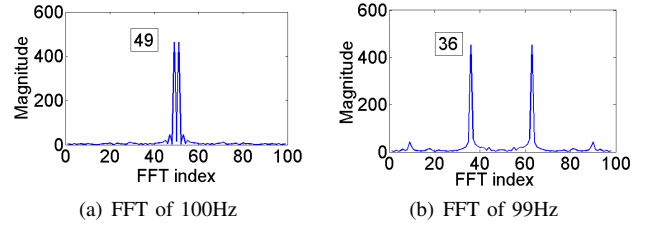


**Fig. 2: FFT results of one 1251Hz LED bulb sampled by ALS at 100Hz and 99Hz. The peaks under 100Hz is (49,51) since  $1251 \bmod 100 = 51$ . The peaks under 99Hz is (36, 63), since  $1251 \bmod 99 = 63$**

### B. Using ALS as a VLC receiver

The VLC by ALS is an under-sampling communication method. As human eyes are sensitive to low rate changes in light intensity, the modulation rate of an LED bulb usually is higher than 1000Hz[7]. However, as mentioned before, the sampling rate of ALS is a 100Hz at most due to the device constraint. From the theory of communication[8], when a high-frequency signal is sampled at a sub-Nyquist rate, the frequency component will be aliased or folded back, which is shown as

$$f_a = \text{Min}(f_t \bmod f_s, f_s - f_t \bmod f_s) \quad (2)$$

where  $f_a$  is the aliased frequency,  $f_t$  is the original frequency and  $f_s$  is the sampling rate. Figure 2 shows the effect of undersampling. Receiving high-frequency signals at a much lower sampling rate is possible.

However, the low frequency is too small to differentiate a large number of frequencies. For example, under the sampling rate of 100Hz, the resolution is only 50, and it can not discriminate the signal of 1001Hz from that of 2001Hz. Actually, from Equation 2, the receiver can only differentiate  $f_s/2$  frequencies with a sampling rate of  $f_s$ . To differentiate these "overlapped" frequencies, we use dynamic sampling rates[9] which the ALS samples the signal multiple times with different sampling rates. With dynamic sampling rates, the resolution of the ALS is improved since the LED flickering frequency has different aliased frequencies under different sampling rates. For example, if the ALS samples the light signal with 100Hz and 99Hz, the signal of 1001Hz will be aliased to 1Hz at 100Hz and 11Hz at 99Hz, and the signal of 2001Hz will be aliased to 1Hz and 21Hz respectively. Therefore, the ALS can differentiate more frequencies. With sampling rates of 100Hz and 99Hz, the resolution of ALS is  $(100/2) * (99/2) = 2475$  which is a considerable improvement. More than two sampling rates can further improve the resolution; however, it causes a longer duration of sampling to decode one frequency as each sampling rate should sample one second. Therefore, we fix the ALS to sample a light signal with two different sampling rates in our following design.

### C. Indoor Localization with ALS

Based on the VLC by ALS, we propose ALS-P, a lightweight VLP system. Figure 3 illustrates the overall system architecture of ALS-P. The VLP scenario we target is similar to traditional indoor localization approaches[2], [10] where there are thousands of LEDs deployed in a building.

The core idea of ALS-P is to use frequencies to represent locations. We note that almost all the LED bulbs(both intelligent and regular ones) use Pulse Width Modulation (PWM), for

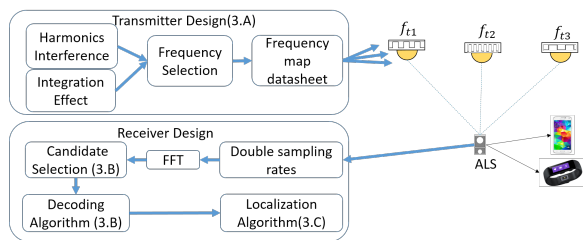


**Fig. 3: The structure of ALS-P**

example, turning on and off LED at specific frequencies and duty cycles, to generate light signals. This is a conventional approach to enable dimming and to compensate for the lighting efficiency loss after long time use. Particularly in our ALS-P system, each LED bulb uses a unique and fixed PWM frequency to generate its light signal, which serves as its identifier. In the localization scenario, mobile devices with ALS are the receivers which install a localization app. The locations of LED bulbs are stored in the localization app. Mobile devices with ALS can identify the flickering frequencies of the LED bulbs, which serves as localization anchors. According to this, mobile devices can infer its location.

### III. SYSTEM DESIGN

In this section, we propose the design of ALS-P including the transmitter, receiver and localization algorithm.

#### A. ALS-P Transmitter Design

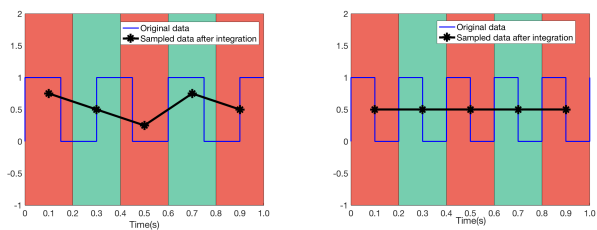
In this section, we propose the design of the ALS-P transmitter, in which the target is to assign frequencies to all the LED bulbs. We will first introduce the challenges in the transmitter design and then propose a frequency selection scheme as a solution. The challenge of transmitter design is that some frequencies cannot be assigned to LED bulbs due to the integration effect and harmonics interference. The frequency selection scheme will handle those effects and generate all the frequencies that can be assigned to LED bulbs.

1) *Handling the Impact of Integration Effect:* The sampling property of ALS and common ADC is different. In common ADC sampling, signals of different frequencies have the same response. However, the response of a signal received by ALS is related to the frequency of the original signal. As shown in Figure 4, the response of 5Hz and that of 3.3Hz are different when the receiver is an ALS. It is caused by the integration effect of the ALS, which has been already mentioned in the Overview Section. The red and green areas in Figure 4 represent the integration duration which is 0.2s. When receiving the 5Hz signal, the sample collected by ALS is always one period of the original signal, and the response is still zero no matter when it starts to do sampling.

To understand the integration effect, we formulate the model of frequency response as follows. Each sample received by ALS in the integration can be expressed as a rectangular window function on the original signal. Assuming that the integration time is  $t_i$  and the ALS sampling model is Equation 1, the output of ALS at time  $t$  can be revised as:

$$A(t) = \int_{-\infty}^{+\infty} I(\tau) \text{rect}(\tau - t) d\tau \quad (3)$$

where  $\text{rect}(\tau - t)$  is the function that evaluates to 1 during  $(t, t + t_i)$  and 0 otherwise. Similar to the process from [10], the



(a) 3.3Hz Data (b) 5Hz Data

**Fig. 4: The example of integration effect. The red and green areas are used to differentiate adjacent integration time zone of ALS. The blue lines are the original signal from LED lights and the black lines are the sampled data by ALS.**

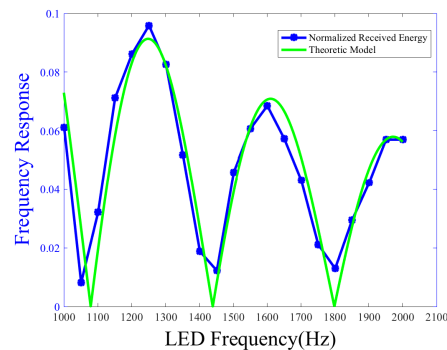


**Fig. 5: Received energy, calculated SNR and the theoretic model of frequency response**

expression after Fourier transform would be

$$F(A) = \int_{-\infty}^{+\infty} I(\tau) e^{-j2\pi f\tau} d\tau \int_{-\infty}^{+\infty} \text{rect}(-T) e^{-j2\pi fT} dT \quad (4)$$

$$= -F(I) \cdot F(\text{rect})$$

Therefore, the response of frequency  $f$  is

$$|H(f)| = \frac{|F(A)|}{|F(I)|} = |F(\text{rect})| = \left| \frac{\sin(\pi f t_i)}{\pi f t_i} \right| = |\text{sinc}(f t_i)| \quad (5)$$

Figure 5 plots the theoretical model of the frequency response and the normalized data from a real experiment in which an ALS sensing lights of different frequencies. According to this figure, there is a vast variation in the response of light among different frequencies. Therefore, due to the integration effect, some frequency signals are difficult to decode when received by an ALS.

We define a threshold  $th_f$  to handle the integration effect. When deciding a frequency of one LED bulb, we should leave out the frequencies with the low-frequency response. Specifically, the frequency  $f$  will be assigned to a LED bulb if

$$|H(f)| \geq th_f \quad (6)$$

where  $H(f)$  is the frequency response function we defined.

2) *Handling the Harmonics Interference:* As mentioned in the Overview Section, the signal generated by each LED bulb is a PWM wave signal. The blue curves shown in Figure 4 are the examples of the signal. As a result, the frequency expression of the PWM wave is a Fourier Series and harmonic waves

accompany the primary wave. The Fourier Series representation of a PWM wave with frequency  $f$  is:

$$x_p(t) = a_0 + \sum_{n=1}^{\infty} (a_n \cos(n \cdot 2\pi ft)) \quad (7)$$

where

$$a_n = 2 \frac{A}{n\pi} \sin(nc\pi) \quad (8)$$

for any  $n > 0$ , where  $A$  is the average magnitude of the original signal and  $c$  is the duty cycle of the PWM wave. We denote that the first order signal, which is  $\sin(2\pi ft)$ , as the primary wave and others as harmonic waves in the rest of the paper. The frequency response of a harmonic wave of one PWM signal should be the production of the response related to the Fourier expression and the gain related to its frequency, which is

$$R_n(f) = |a_n \cdot H(nf)| = 2 \frac{A}{n\pi} |\sin(nc\pi) \text{sinc}(nft_i)| \quad (9)$$

for any  $n > 0$ , where  $R_1(f)$  is the response of the primary wave and others are that of harmonic waves.

The harmonics interference is possible in two scenarios. First, the response of the harmonic wave may overcome that of the primary wave. Second, when multiple LED bulbs existed, the power of a harmonic wave of an LED bulb with a strong frequency response may be comparable or even stronger than the primary wave of an LED bulb with a weak response frequency. Both effects may lead to error in aliased frequency detection and further affect the decoding algorithm.

According to the derivation, the first concern never exists in our model. For any  $n > 1$ , we have

$$\frac{|a_n|}{|a_1|} = \frac{|2 \frac{A}{n\pi} \sin(nc\pi)|}{|2 \frac{A}{\pi} \sin(c\pi)|} = \frac{|\sin(nc\pi)|}{n|\sin(c\pi)|} \quad (10)$$

Based on the axiom that  $|\sin(nx)| \leq n|\sin(x)|$  for any  $x$  and integer  $n$ , we have

$$|a_n| \leq |a_1| \quad (11)$$

for any  $n \geq 1$  and duty cycle  $c$ . Similarly, since  $|H(nf)| = \frac{|\sin(nf\pi)|}{nf\pi}$ , with the same axiom we have

$$|H(nf)| \leq |H(f)| \quad (12)$$

for any  $n \geq 1$ . As a result,

$$R_n(f) \leq R_1(f) \quad (13)$$

for any  $f$  and  $n \geq 1$ . As a result, the frequency response of every harmonic wave is not higher than that of the primary wave of the PWM wave with any frequency and duty cycle.

On the other hand, the second concern is possible owing to the variable responses among different frequencies. Our solution to address this problem is to select the frequencies with weak harmonic waves. In Equation 9, the model of harmonic waves, the parameter  $a_n$  is related to the duty cycle and  $H(nf)$  is associated with the primary frequency and the order. We define a threshold  $th_h$  to select the frequencies with weak harmonic responses. A frequency has a weak response when the following condition is matched.

$$|H(nf)| \leq th_h |H(f)| \quad (14)$$

Aliased Frequency at 100Hz	Aliased Frequency at 99Hz	Original Frequency(Hz)	Geographical Location
1	11	1001	(a,b,c)
2	12	1002	(d,e,f)
●			
●			
●			
20	31	1120	(g,h,i)
20	32	1220	(j,k,l)
●			
●			
●			

Fig. 6: Example of the frequency map datasheet

for any  $n > 1$ . Then we have

$$R_n(f) = |a_n \cdot H(nf)| \leq |a_0| (th_h |H(f)|) = th_h R_1(f) \quad (15)$$

Under such conditions, the harmonic waves of such signals are insignificant to the primary wave. Since we have limited the lowest power of the primary wave when handling integration effect, the second concern can be avoided when the strongest harmonic wave is still weaker than the signal with the lowest response, which is achievable with  $th_f$  and  $th_h$ .

3) *Frequency Selection System*: The frequency selection system is design based on the effects of integration and harmonic. It includes two steps, frequency map datasheet generation and frequency assignment.

The frequency map datasheet generation is to construct a list that each frequency in the list can be assigned to the ALS-P transmitter, the LED bulb. First, all the integral frequencies from 1000Hz to the highest frequency that the LED bulb can reach are checked with the two thresholds. As a result, we can get a set of frequencies  $S$  that

$$S = \{f \mid |H(f)| > th_f \ \& \ |H(nf)| \leq th_h |H(f)| (\forall n > 1)\} \quad (16)$$

Based on  $S$ , we generate the corresponding datasheet. The example of the data sheet is shown in Figure 6. Each row represents one frequency and its aliased frequencies on the two sampling rates. It is possible that multiple frequencies in  $S$  have the identical aliased frequencies on the two sampling rates. In this condition, we preserve the frequency with the highest response and delete the others.

The frequency assignment is to randomly assign one unique frequency from the datasheet to one LED bulb in the building. Since each LED bulb has its global position in the building, we further add the location information in the datasheet as shown in Figure 6.

## B. ALS-P Receiver Design

The receiver design includes two parts, the decoding algorithm, and the environmental effects prevention. The decoding algorithm is proposed to decode the frequency of each LED bulb based on the sensing data from ALS. In the second part, we consider the effect of fluorescent light on receiver decoding and then propose the mechanism to handle it.

1) *Decoding Algorithm*: The job of the decoding algorithm is to generate the IDs of all LED bulbs whose lights are sensed by ALS. Its input is the FFT results of the sampling data by ALS under two sampling rates. The approach of the decoding algorithm is first to find the indexes with high magnitude from the FFT results as the candidates of the aliased frequencies by

a procedure called candidate selection. Then, the frequency of each LED bulb is decoded by picking up one frequency in the candidates of each sampling rate and pairing them to search in the frequency map datasheet.

The candidate selection in one FFT result is to find all the candidates of aliased frequencies which is to select the index with high magnitude from the FFT. The method is based on the magnitude index in the FFT result. We define a threshold  $th_d$  in the candidate selection. Suppose that the FFT result is  $\{F_s(i)\}$  in which  $i$  is the FFT index,  $s$  is the sampling rate and  $F(i)$  is the corresponding magnitude. The index  $i$  will be selected as a candidate of aliased frequencies if

$$F(i) \geq th_d \cdot \max(F(i)) \quad (17)$$

As a result, we have two sets of candidates from the FFT results of two sampling rates.

The decoding is challenging with the two sets since we do not know how to pair the elements in the two sets. The result of the decoded frequencies can be different with different combination pairs. For example, suppose that the candidates are 1Hz, 3Hz at a 100Hz sampling rate and 13Hz, 15Hz at a 99Hz. If we pair 1Hz and 13Hz and pair 3Hz and 15Hz, we will get 1201Hz and 1203Hz. However, if we pair 1Hz and 15Hz and pair 3Hz and 13Hz, we will get 1401Hz and 1003Hz, which is entirely different from the previous result. This problem is much worse with more than 2 LED bulbs. To handle this problem, we utilize the observation that each LED has its unique location and the sensed multiple lights must be nearby geographically. We can search all the possible combinations of LED frequencies and find one within a small area in the geography with a threshold  $th_{dis}$ . The combination is valid if the distance of any pair of LED bulbs in the combination is shorter than  $th_{dis}$ . In specific, the set of decoded frequency  $D = \{f\}$  is valid if

$$dis(f_1, f_2) \leq th_{dis}, \forall f_1, f_2 \in D \quad (18)$$

where  $dis(i, j)$  is the distance between the LED with frequency  $i$  and  $j$  in the geography, and the location information is obtained from the frequency map datasheet.

2) *Environmental Effects*: In practice, the LED bulbs are not the only light source in the building since the fluorescent lights are still widely deployed. The existence of the fluorescent light affects the decoding accuracy of ALS-P since fluorescent lights have a fixed frequency of 50Hz or 60Hz according to the AC configuration. As a result, when there are fluorescent lights deployed, the aliased frequency of them are also detected by ALS. However, since the frequency index of fluorescent light is fixed in each country, we can handle it by leaving out the specific frequencies.

There are two possible conditions with fluorescent lights. One is that a real aliased frequency by a LED bulb at the frequency of the fluorescent light, the other is not. We revise the decoding algorithm by considering both conditions. The algorithm will first search with the assumption that there is no overlapped frequency. If no valid combination is generated, the algorithm will consider the overlapped scenario.

In our design, the algorithm can generate multiple answers at some time. However, since the frequencies of all LED bulbs are assigned at random, the possibility of multiple answers is very low. We show the results in the Evaluation Section.

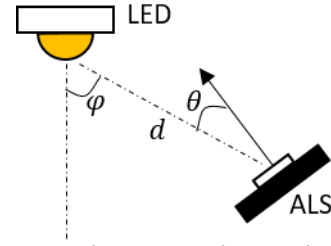


Fig. 7: The optical model in localization algorithm

### C. Localization Algorithm

After decoding the frequencies of all LED bulbs, the last step is localizing the receiver position. The principle of the localization algorithm of ALS-P is trilateration. When the frequency of each LED bulb has been decoded, ALS-P also gets its location information and the received energy. The location information each LED bulb is the global 3-D coordinates from the frequency map datasheet. The received energy is the magnitude of its aliased frequency on the FFT results which is related to multiple parameters such as distance to the LED bulb, the irradiation angle of the LED bulb, the incidence angle of the ALS and duty cycle of the signal. Its model in ALS-P scenario is similar to the optical model of existing VLP systems [11] except that we also consider the frequency response. As a result, the RSS measured of one LED bulb is

$$P_r = A|H(f)|\sin(c\pi)\frac{p(\theta)q(\phi)}{d^2}; \quad (19)$$

where  $P_r$  is the received power which is estimated by the magnitude from FFT,  $A$  is the constant related to its maximum emission power,  $f$  is the LED bulb frequency,  $c$  is the duty cycle,  $p(\theta)$  is the incidence angle response function of the ALS,  $q(\phi)$  is the irradiation angle response function of the LED bulb and  $d$  is the distance between the LED bulb and the receiver. In those parameters,  $\theta$ ,  $\phi$  and  $d$  are related to the location of the receiver, which is a 3-D value as shown in Figure 7.

Based on the model, our localization algorithm is designed as a Levenberg-Marquardt optimization process[12]. We do not provide the details of the localization algorithm since it is not our contribution. As a whole, the localization algorithm needs at least 3 LED bulbs to solve the problem.

## IV. IMPLEMENTATION

The implementation of ALS-P includes hardware configuration and software implementation.

### A. ALS-P Hardware

We choose TMG3992, the ambient light sensor from ams[6], as the prototype ALS of ALS-P which has been equipped by a series of Samsung smartphones such as Note 4, Galaxy S5 and Galaxy S6. The minimum integration time of TMG3992 is 2.78ms, and the maximum sampling rate is 100Hz. Since most of the smartphone operating systems do not provide the API of the ALS configuration, we directly control the ALS by an Arduino board. In future, it is simple for manufacturers to implement ALS-P on a commercial smart device by opening corresponding APIs. We control the ALS by Arduino Uno[13] and set it with the minimum integration time, as shown in Figure 8. We set the sampling rates as 100Hz and 99Hz, and

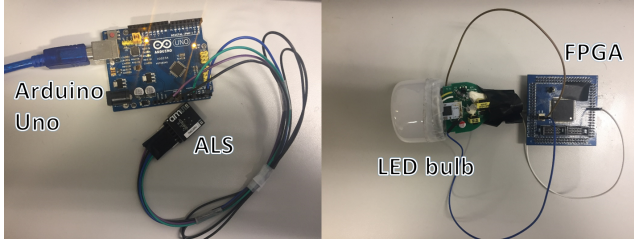


**Fig. 8: Photos of ALS-P components.**

the sampling duration is 1 second under each sampling rate. As a result, the total sampling duration is 2 seconds.

The prototype of the LED bulb in ALS-P is the YEELIGHT LED Bulb[14] controlled by Alter Cyclone 2 FPGA. It supports pulse wave with a frequency from 1000Hz to 3000Hz with variable duty cycles.

### B. ALS-P Software

In the transmission design part, the frequency selection scheme needs to determine two thresholds  $th_f$  and  $th_h$ . According to Equation 5, the max frequency response of TMG3992 is 0.0913 when  $f > 1000$ . Therefore, we set the thresholds to  $th_f = 0.02$  and  $th_h = 0.2$ . Based on those thresholds, we generate the frequency map datasheet. Since the frequency range of the YEELIGHT is from 1000Hz to 3000Hz, the size of the generated datasheet is 1179 when the sampling duration is 2 seconds in total. According to [5], the number of LED bulbs in a typical building is less than 400; thus the generated datasheet is sufficient for the localization purposes in practical with both sampling durations.

In the receiver design part, we implement the sensing, FFT, decoding algorithm in the Arduino board and run the localization algorithm offline on Matlab. The decoding algorithm utilizes the threshold  $th_d$  to select candidates for aliased frequencies. As the threshold to handle harmonics interference  $th_h$  is 0.2, we also let  $th_d = 0.2$  in the implementation to accord with the design of the transmitter. The threshold of decoding frequencies  $th_{dis}$  is denoted as  $4m$ .

## V. EVALUATION

### A. Evaluation Overview

The evaluation includes two parts: ALS-P decoding performance and localization result. For the ALS-P decoding performance, we evaluate the decoding performance and interference resistance of ALS-P in various scenarios. It is the main part of the evaluation which includes experiments with a single LED bulb, multiple LED bulbs, variant frequencies, and different environmental effects. We also analyze the data throughput of ALS-P in this part. In the localization evaluation, we analyze the localization accuracy of our proposed system. The localization evaluation assumes that we have successfully decoded frequencies of all received LED bulbs and it uses the location information and the received energy as the input of the localization algorithm. For the purpose of localization evaluation is to verify the ALS-P's application, we set up a small area testbed to do the localization evaluation.

### B. ALS-P Decoding Performance

1) *Single LED bulb*: In this subsection, we evaluate the decoding performance of ALS-P, which is the most important

part of the evaluation, since the decoding performance determines the accuracy of localization. The decoding performance depends on two factors, the accuracy of choosing aliased peaks generated by LED bulbs in FFT results and the accuracy of decoding frequencies of LED bulbs based on the indexes of the chosen peaks.

The accuracy of choosing aliased peaks requires the aliased peaks have more significant power than other noise peaks. Based on [10], we set the 3dB as the SNR threshold for the aliased peaks where the noise is the highest power of the peaks except all aliased peaks. We evaluate it under a single LED bulb, multiple LED bulbs, ambient effects and mobility scenarios. In all cases, the duty cycle is 50%, and the ALS senses the light under 100Hz and 99Hz for five times to get the average result in the evaluation.

We first evaluate the performance of aliased peaks under a single LED bulb with different distances and frequencies which shows the essential part of ALS-P design. We deploy a LED bulb at a specific location and then change the frequency of its light. For each frequency, we move the ALS from 0.5m to 4m in a straight line towards the LED bulb to measure the SNR of the aliased peaks in the FFT results. Figure 9 shows the received power strength versus distance under the frequencies of 1036Hz, 1503Hz and 1723Hz where the three frequencies have similar frequency response based on 5. The result under frequencies with different frequency response is shown in Figure 10 where 1251Hz, 1762Hz and 1799Hz are assigned and their frequency responses are:  $H(1036) = H(1503) = H(1723) = 0.04$ ;  $H(1251) = 0.09$ ,  $H(1762) = 0.02$  and  $H(1799) = 0.00024$ . Based on both results, the received power strength falls off against the distance by square as expected. Besides, the frequency response model is verified as the lights with similar frequency response have similar results. Figure 11 shows the result of SNR versus distance with those frequencies, in which we can find that the distance doesn't affect the SNR since the noise peak is also weak at a long distance. Besides, the signal with poor frequency response is inclined to have a lower SNR. But as a whole, the SNR will be larger than 3dB with a proper frequency response within 4 meters which is a reasonable transmission range in practice.

2) *Multiple LED bulbs*: In this part, we evaluate decoding performance with multiple LED bulbs to verify the ALS-P's capability of receiving frequencies from multiple LED bulbs simultaneously. We first evaluate ALS-P with two LED bulbs in which the two LED bulbs are deployed at the ceiling with 1.5m apart. We choose three frequencies, 1251Hz which has a good frequency response, 1723Hz which has an average frequency response and 1799 which has a bad frequency response and assign any two of them to the LED bulbs. For each combination, the ALS moves horizontally under the ceiling from the LED bulb with a higher frequency response to the LED bulb with lower frequency response and the height between ALS and LED is 2m. As shown in 12, the frequency with a bad response always has a negative SNR when there is another LED bulb with a higher response frequency at any locations even though its SNR is getting better as ALS moves to the corresponding LED bulb. It is because that its received energy is too weak compared with the signal with higher frequency response. Therefore, it is reasonable to select frequencies with good responses based on  $th_f$  to be assigned to LED bulbs. Besides, the LED bulbs

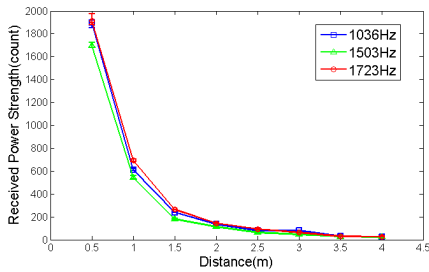


**Fig. 9: Received power versus distance with similar frequency responses**

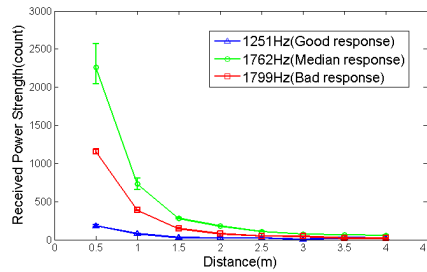


**Fig. 10: Received power versus distance with different frequency responses**

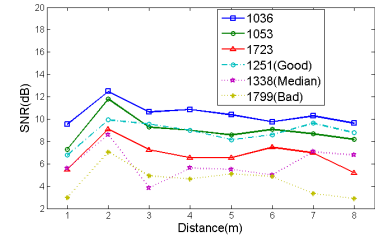


**Fig. 11: The SNR versus distance results**

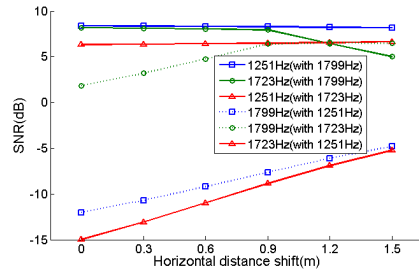


**Fig. 12: The SNR under dual LED bulbs with different combination of frequencies**

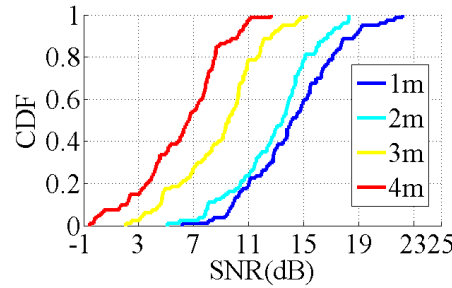


**Fig. 13: CDF of the multiple LED SNR under different distance**

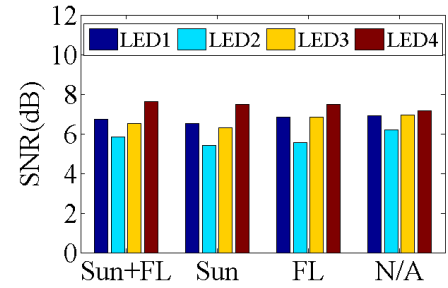


**Fig. 14: The ambient effect performance**

with an average frequency response maybe not detected when it is too far away as shown in the lines with circles of 12. The light of 1723Hz is less than 3dB when ALS is just under the light of 1251Hz. Therefore the decoding algorithm can only select the aliased peaks of 1251Hz. However, in such situation, the user must under the LED bulb which is helpful to the localization algorithm. As a result, even though it is possible that some LED bulbs have a low SNR with a higher response frequency light because of the lower limit frequency response in our implementation, the localization algorithm can still be able to get an accurate result based on the aliased inputs.

Then we extend the evaluation to the scenario of 4 LED bulbs. The 4 LED bulbs are deployed on a board with a shape of a square, and the square length is 1.5m. We randomly assign four frequencies to 4 LED bulbs for 20 times based on the frequency map datasheet in our implementation. Each time we measure the SNR at a distance from 1m to 4m, where the distance is from the ALS to the center of the square. The whole CDF plot is shown in Figure 13, in which we find that a better SNR is achieved in a shorter distance. Nearly 85% of the lights have an SNR higher than 3dB even at a distance of 4m. Therefore under multiple LEDs, ALS-P has a good VLC performance within 4 meters.

3) *Ambient effect and mobility:* In this part, we first evaluate the impact of ambient light and the performance of receiving by measuring the data of 4 LED bulbs in different environments. We randomly assign one frequency to each LED and evaluate the SNR under the sunlight, fluorescent light or both of them. The 4 LED bulbs are deployed as the previous setup, and the distance is 3 meters. The results are shown in Figure 14. We can find that the SNR of 4 LEDs remains steady with different ambient light scenarios. For the scenario with the fluorescent light, the SNR calculation ignores the FFT peak caused by

the fluorescent. It shows that the sunlight has little impact on ALS-P and our decoding algorithm can handle the interference of the fluorescent light.

Then, we evaluate the effect of mobility under different distances. Even though there is no specific design to handle the mobility effect in ALS-P design, we still want to evaluate it to see the performance under mobility. In this setup, one LED bulb is deployed on the ceiling, and the ALS will be moving horizontally at different heights. We measure the decoding performance under multiple movements: steady, slow motion and fast motion, where the slow motion is imitating walking, and the fast one mimics running. In the slow motion, the ALS will be moving at speed around 1m/s, and in the fast one, the ALS will be moving around 2m/s. In all scenarios, the ALS is facing up to the ceiling. Figure 15 shows the sample FFT results under the three scenarios, in which we can find that the noise of 1Hz is more significant with a faster speed. Figure 16 is the SNR result except 1Hz which shows that ALS-P still performs similarly to the steady condition when the user is walking and is still able to decode when the user is running, which validates the effectiveness of handling mobility. It is noticeable that the performance of fast motion increases when the distance increases. The reason is that the ALS may move out of the LED bulb emission areas by fast movement at a closer distance where it may not see the LED bulb lights. At a further distance, the ALS can better remain in the view of LED bulbs, and the SNR is increased. In this evaluation, we guarantee that the aliased frequencies of the LED bulb are not too small (e.g., 1Hz or 2Hz), which may lead to interference. We expand on it in the Discussion Section.

4) *Decoding accuracy simulation:* In this part, we evaluate the robustness of the decoding algorithm via a simulation of Matlab. We draw a virtual map of 20m × 25m, and each LED

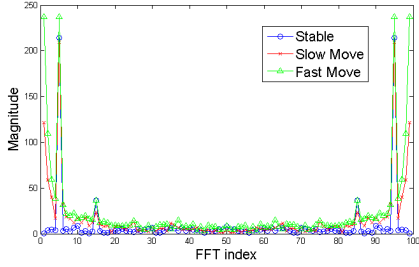


Fig. 15: The FFT results under different mobility scenarios

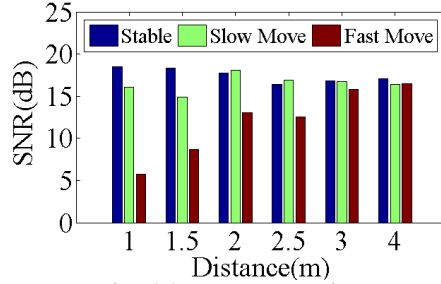


Fig. 16: The evaluation of mobility

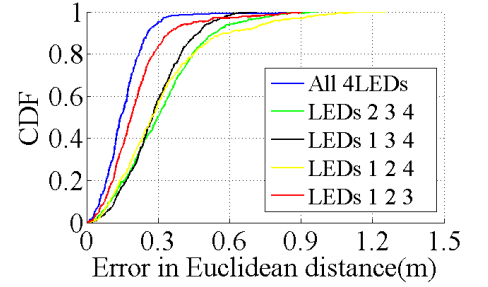


Fig. 17: CDF of the localization error

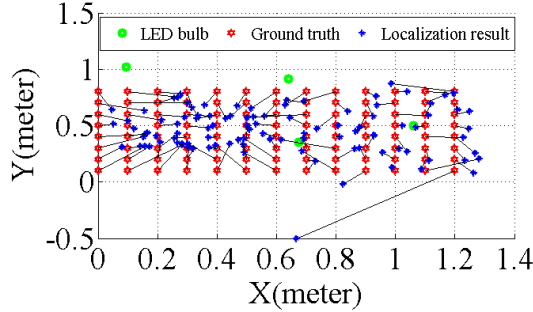


Fig. 18: The visualization of localization error(4 LED bulbs)

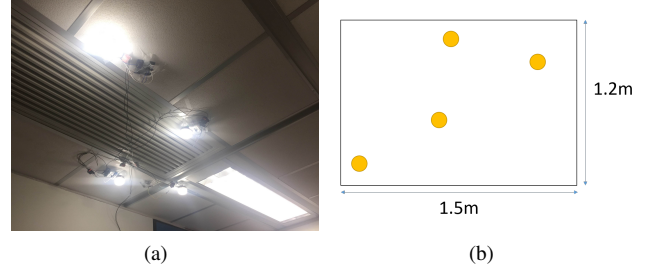


Fig. 19: The testbed for localization evaluation. (a) is the implementation and (b) is the conventional diagram of 4 LED bulbs

is deployed on the integral coordinates. As a result, there are 500 LED bulbs in total. For each round, each LED bulb will be assigned with a unique frequency based on the frequency map datasheet, and the ALS will be under each LED bulb one by one to try to detect the nearby frequencies based on the received aliased frequencies. At each location, we denote the sensing range of ALS as a circle with a radius of  $r_{dis}$  and to see whether there is a collision of decoding. The collision happens when the ALS can get the same aliased frequencies at a location elsewhere with the same radius. We simulate for 1000 times and let  $r_{dis}$  to be  $4m$  at most, and the number of collisions is zero under all conditions. The simulation result shows that the decoding algorithm can achieve an accurate result given the correct aliased frequencies as the input and it is reasonable to set the  $th_{dis}$  as  $4m$  in ALS-P implementation.

5) *Data throughput*: ALS-P can decode the high frequencies with dual sampling rates. In our implementation, the size of the generated datasheet is 1179 under sampling duration of 2 seconds. Therefore, under the scenario of a single LED bulb, the transmission capacity of ALS-P is about 10bits for 2 seconds which is 5bit/s. The data throughput increases with multiple LED bulbs and we will enable low data communication of ALS-P in our future work.

### C. Localization Evaluation

In this section, we evaluate the localization accuracy of ALS-P localization algorithm using the testbed shown in Figure 19. There are 4 LED bulbs deployed on the ceiling of the room with an area about  $1.5m \times 1.2m$ . The height distance between the test bed and ALS is  $1.5m$ , and we assume that the orientation of the ALS is towards the ceiling. We move ALS to do positioning and scan the total area with a step size of  $10cm$  under the testbed. The whole CDF plot is shown in Figure 17. With 4 LEDs, ALS-P can achieve an accuracy of  $15cm$  at 50%

under our testbed, and  $25cm$  at 90%. Figure 18 also shows the visualized map of localization result. As a result, ALS-P provides a sub-meter level of accuracy with at least 4 LEDs. We also evaluate the ALS-P performance with 3 LEDs, which is also shown in Figure 17, from which we find that the accuracy decreases with the fewer number of LED bulbs. However, the decimeter level accuracy is still good for general localization requirements.

## VI. RELATED WORK

**Visible Light Communication.** VLC has been studied with different context and design goals. Typical VLC research aims to provide a communication channel with high throughput [15], [16], [17], rate adaptation [18], and capability of dark transmission [1]. They need high functional photodiode as the receiver to sense the modulated light signal which is different from our goal. We focus on providing an energy-efficient VLP system for commercial smartphones or resource-constrained mobile devices without any modifications.

**Visible Light Localization** The VLP is a typical application of VLC. Recent studies[2], [19], [11] show that visible light based localization is a promising approach with higher accuracy since visible light is more directional and stable. The difference between existing work and ALS-P is the system requirements of the end user. Most of the works[10], [3], [2], [20], [21] utilize the camera as the receiver and achieve sub-meter level accuracy based on the rolling shutter effect. However, the power consumption is high for camera viewing and capturing. Some works[11], [22], [23] exploit the traditional light sensor as the receiver or make a particular modification. The most related work is [4] which also utilize the ambient light sensor to achieve high accuracy localization, however, it requires dual-ALS which is not a standard setup in commercial smartphones. In contrast, ALS-P uses the general ambient light sensor from commercial smartphones or wearables.

**Sparse Sensing** ALS-P shares the idea of sparse sensing with other works on wireless signal[9], [24]. They exploit the sparsity of the frequency domain to sample the signal overcome the limitation of the Nyquist theorem. However, there are unique challenges in the visible light domain such as LED selection and the interference. Therefore we propose several new schemes to overcome such challenges and optimize the power consumption.

## VII. DISCUSSION AND FUTURE WORK

### A. Decoding Error

We have verified that the possibility of getting errors in decoding algorithm is rarely based on Matlab simulation. However, there is a possibility that the decoding algorithm can not result in a legal output when the number of observed aliased frequencies is less than the number of sensed lights. In other words, the nearby LED bulbs may share the same aliased frequencies. For example, there are 4 LED bulbs, but there are only two aliased frequencies under each sampling rate. As a result, even though we can decode some frequencies accurately based on the input, we can not get the real power strength of each LED bulb which leads error in the localization algorithm. Since the possibility of such a scenario is minimal and owing to the limitations of the paper, we do not propose a scheme to handle such a problem. In future work, we will delve into such a problem to make ALS-P more comprehensive.

### B. Human Mobility

ALS-P evaluates the performance with human mobility. When the ALS is moving, the power of received signals will waver as the distance between the ALS and LED bulbs changes. Therefore, there is low-frequency noise in the FFT result which is due to the movement. As a result, the aliased frequencies will not experience interference when they are, for example, larger than 2Hz, which is the configuration in the Evaluation Section. This problem is similar to the fluorescent light effect, which has a noise signal at a fixed position in the FFT result. In the future, we can deal with this problem by checking the power of the low-frequency indexes in the FFT result.

### C. Data Communication

In the evaluation section, we analyze the data throughput of ALS-P based on calculation. One LED bulb can transmit data by changing its shaking frequencies by time and broadcast some information. ALS-P is possible to support a low data rate communication which needs further designs for encoding and synchronization. It can enable applications in reality such as broadcasting in museums or parking lots. We will leverage such designs in our future work.

## VIII. CONCLUSION

In this paper, we present the system design of ALS-P, which provides a lightweight, visible light communication scheme for smartphones and wearables. The idea is to utilize the under-sampling of ALS to detect the high-frequency of LED bulbs. To address the design challenges, ALS-P enables a transmitter design to select suitable frequencies for LED and receiver design to handle the interference in practical. We implement a prototype of ALS-P by utilizing existing sensors of commercial devices and a prototype of a localization and tracking system to show its application. The experiments validate our idea as well as the system design.

## REFERENCES

- [1] Z. Tian, K. Wright, and X. Zhou, "The darklight rises: Visible light communication in the dark," in *Proceedings of the 22nd Annual International Conference on Mobile Computing and Networking*. ACM, 2016, pp. 2–15.
- [2] Y.-S. Kuo, P. Pannuto, K.-J. Hsiao, and P. Dutta, "Luxapose: Indoor positioning with mobile phones and visible light," in *Proceedings of the 20th annual international conference on Mobile computing and networking*. ACM, 2014, pp. 447–458.
- [3] Z. Yang, Z. Wang, J. Zhang, C. Huang, and Q. Zhang, "Wearables can afford: Light-weight indoor positioning with visible light," in *Proceedings of the 13th Annual International Conference on Mobile Systems, Applications, and Services*. ACM, 2015, pp. 317–330.
- [4] C. Zhang and X. Zhang, "Pulsar: Towards ubiquitous visible light localization," in *Proceedings of the 23rd Annual International Conference on Mobile Computing and Networking*. ACM, 2017, pp. 208–221.
- [5] S. Zhu and X. Zhang, "Enabling high-precision visible light localization in today's buildings," in *Proceedings of the 15th Annual International Conference on Mobile Systems, Applications, and Services*. ACM, 2017, pp. 96–108.
- [6] "Ams tmg399x," [http://ams.com/eng/content/download/664463/1748297/file/TMG3992\\_Datasheet\\_EN\\_v2.pdf](http://ams.com/eng/content/download/664463/1748297/file/TMG3992_Datasheet_EN_v2.pdf), Mar 2017.
- [7] R. Chase, "The initiation and conduction of action potentials in the optic nerve of tritonia," *Journal of Experimental Biology*, vol. 60, no. 3, pp. 721–734, 1974.
- [8] A. Antoniou, *Digital signal processing*. McGraw-Hill Toronto, Canada, 2006.
- [9] H. Hassanieh, L. Shi, O. Abari, E. Hamed, and D. Katabi, "Ghz-wide sensing and decoding using the sparse fourier transform," in *INFOCOM, 2014 Proceedings IEEE*. IEEE, 2014, pp. 2256–2264.
- [10] C. Zhang and X. Zhang, "Litell: robust indoor localization using unmodified light fixtures," in *Proceedings of the 22nd Annual International Conference on Mobile Computing and Networking*. ACM, 2016, pp. 230–242.
- [11] L. Li, P. Hu, C. Peng, G. Shen, and F. Zhao, "Epsilon: A visible light based positioning system," in *NSDI*, 2014, pp. 331–343.
- [12] J. J. Moré, "The levenberg-marquardt algorithm: implementation and theory," in *Numerical analysis*. Springer, 1978, pp. 105–116.
- [13] "Arduino uno," <https://www.arduino.cc/en/Main/ArduinoBoardUno>, Mar 2017.
- [14] "Yeelight led bulb (white)," [https://www.yeelight.com/en\\_US/product/wifi-led-w](https://www.yeelight.com/en_US/product/wifi-led-w), Mar 2017.
- [15] T. Komine and M. Nakagawa, "Fundamental analysis for visible-light communication system using led lights," *IEEE transactions on Consumer Electronics*, vol. 50, no. 1, pp. 100–107, 2004.
- [16] Y. Wang, Y. Wang, N. Chi, J. Yu, and H. Shang, "Demonstration of 575-mb/s downlink and 225-mb/s uplink bi-directional scm-wdm visible light communication using rgb led and phosphor-based led," *Optics express*, vol. 21, no. 1, pp. 1203–1208, 2013.
- [17] S. Schmid, G. Corbellini, S. Mangold, and T. R. Gross, "Led-to-led visible light communication networks," in *Proceedings of the fourteenth ACM international symposium on Mobile ad hoc networking and computing*. ACM, 2013, pp. 1–10.
- [18] J. Zhang, X. Zhang, and G. Wu, "Dancing with light: Predictive in-frame rate selection for visible light networks," in *Computer Communications (INFOCOM), 2015 IEEE Conference on*. IEEE, 2015, pp. 2434–2442.
- [19] N. Rajagopal, P. Lazik, and A. Rowe, "Visual light landmarks for mobile devices," in *Proceedings of the 13th international symposium on Information processing in sensor networks*. IEEE Press, 2014, pp. 249–260.
- [20] M. Yoshino, S. Haruyama, and M. Nakagawa, "High-accuracy positioning system using visible led lights and image sensor," in *Radio and Wireless Symposium, 2008 IEEE*. IEEE, 2008, pp. 439–442.
- [21] H.-Y. Lee, H.-M. Lin, Y.-L. Wei, H.-I. Wu, H.-M. Tsai, and K. C.-J. Lin, "Rollinglight: Enabling line-of-sight light-to-camera communications," in *Proceedings of the 13th Annual International Conference on Mobile Systems, Applications, and Services*. ACM, 2015, pp. 167–180.
- [22] B. Xie, G. Tan, and T. He, "Spinlight: A high accuracy and robust light positioning system for indoor applications," in *Proceedings of the 13th ACM Conference on Embedded Networked Sensor Systems*. ACM, 2015, pp. 211–223.
- [23] S.-Y. Jung, S. Hann, and C.-S. Park, "Tdoa-based optical wireless indoor localization using led ceiling lights," *IEEE Transactions on Consumer Electronics*, vol. 57, no. 4, 2011.
- [24] H. Hassanieh, P. Indyk, D. Katabi, and E. Price, "Simple and practical algorithm for sparse fourier transform," in *Proceedings of the twenty-third annual ACM-SIAM symposium on Discrete Algorithms*. Society for Industrial and Applied Mathematics, 2012, pp. 1183–1194.